Research Article | Vol. 24, No. 21 | 17 Oct 2016 | OPTICS EXPRESS 23707

Optics EXPRESS

Common phase error estimation in coherent optical OFDM systems using best-fit bounding box

TIANWAI BO AND CHUN-KIT CHAN*

Department of Information Engineering, The Chinese University of Hong Kong, Shatin, N.T., Hong Kong SAR, China

*ckchan@ie.cuhk.edu.hk

Abstract: In this paper, we investigate and characterize a new approach of adopting best-fit bounding box method for common phase error estimation in coherent optical OFDM systems. The method is based on the calculation of the 2-D convex hull of the received signal constellation, which is generally adopted in image processing area to correct the skew of images. We further perform detailed characterizations including root mean square error analysis, laser linewidth tolerance, noise tolerance, and computation complexity analysis, via numerical simulations and experiments. The results show the proposed method achieves much improved spectral efficiency and comparable system performance than the pilot-aided method, while it exhibits good estimation accuracy and reduced complexity than the blind phase searching method.

OCIS codes: (060.1660) Coherent communications; (060.2330) Fiber optics communications.

References and links

1. S. Chandrasekhar, X. Liu, B. Zhu, and D. Peckham, "Transmission of a 1.2-Tb/s 24-carrier no-guard-interval coherent OFDM superchannel over 7200-km of ultra-large-area fiber," in Proceedings of the European Conference of Optical Communications (OFC) (2009).
2. S. Wu and Y. Bar-Ness, "OFDM systems in the presence of phase noise: consequences and solutions," IEEE Trans. Commun. **52**(11), 1988–1996 (2004).
3. S. Jansen, I. Morita, T. Schenk, N. Takeda, and H. Tanaka, "Coherent optical 25.8-gb/s OFDM transmission over 4160-km SSMF," J. Lightwave Technol. **26**(1), 6–15 (2008).
4. Z. Liu, J. Kim, D. Wu, D. Richardson, and R. Slavik, "Homodyne OFDM with optical injection locking for carrier recovery," J. Lightwave Technol. **33**(1), 34–41 (2015).
5. X. Yi, W. Shieh, and Y. Tang, "Phase estimation for coherent optical OFDM," IEEE Photonics Technol. Lett. **19**(12), 919–921 (2007).
6. Y. Ha and W. Chung, "Non-data-aided phase noise suppression scheme for CO-OFDM systems," IEEE Photonics Technol. Lett. **25**(17), 1703–1706 (2013).
7. T. Bo, L. Huang, and C. Chan, "Common phase estimation in coherent OFDM system using image processing technique," IEEE Photonics Technol. Lett. **27**(15), 1597–1600 (2015).
8. T. Bo and C. Chan, "Common phase error estimation for coherent optical OFDM system using best-fit bounding box," in Proc. International Conference on Photonics in Switching (IEEE, 2015), pp. 327–329.
9. B. Yuan, L. K. Kwoh, and C. L. Tan, "Finding the best-fit bounding boxes," in Proc. Int. Conf. on Document Analysis Sys. (Springer-Verlag, 2006), pp. 268–279.
10. H. Freeman and R. Shapiral, "Determining the minimum-area encasing rectangle for an arbitrary closed curve," ACM Commun. **18**(7), 409–413 (1975).
11. G. Toussaint, "Solving geometric problems with the rotating calipers," in Proc. IEEE MELECON (1983) **83**, A-10.
12. S. Har-Peled. "On the expected complexity of random convex hulls," Technical Report, 330/98 (1998).
13. R. Atanassov, P. Bose, M. Couture, A. Maheshwari, P. Morin, M. Paquette, M. Smid, and S. Wuhrer, "Algorithms for optimal outlier removal," J. Discrete Algorithms **7**(2), 239–248 (2009).
14. T. Pfau, S. Hoffmann, and R. Noe, "Hardware-efficient coherent digital receiver concept with feedforward carrier recovery for M-QAM constellations," J. Lightwave Technol. **27**(8), 989–999 (2009).
15. R. L. Graham, "An Efficient Algorithm for Determining the Convex Hull of a Finite Planar Set," Inf. Process. Lett. **1**(4), 132–133 (1972).
16. T. M. Chan, "Optimal output-sensitive convex hull algorithms in two and three dimensions," Discrete Comput. Geom. **16**(4), 361–368 (1996).
17. S. G. Akl and G. T. Toussaint, "A fast convex hull algorithm," Inf. Process. Lett. **7**(5), 219–222 (1978).

#273701 http://dx.doi.org/10.1364/OE.24.023707
Journal © 2016 Received 11 Aug 2016; revised 24 Sep 2016; accepted 24 Sep 2016; published 3 Oct 2016

Optics EXPRESS

18. L. Devroye and G. T. Toussaint, "A note on linear expected time algorithms for finding convex hulls," Computing **26**(4), 361–366 (1981).
19. T. M. Schmidl and D. C. Cox, "Robust frequency and timing synchronization for OFDM," IEEE Trans. Commun. **45**(12), 1613–1621 (1997).

1. Introduction

Coherent optical orthogonal frequency division multiplexing (CO-OFDM) is a promising technique enabling next-generation terabit-per-second, bandwidth-variable elastic optical network [1]. It exhibits a superb resilience to the chromatic dispersion and polarization mode dispersion, but is very susceptible to laser phase noise and fiber nonlinearity, due to its long symbol duration. In general, laser phase noise introduces two effects on the optical OFDM signal, including common phase error (CPE) and inter-carrier interference (ICI) [2], which severely degrade the system performance, therefore they have to be carefully estimated and compensated.

Compensation of CPE in coherent optical systems has been studied extensively, and in general, there have been two common approaches reported, namely analog approaches based on radio frequency (RF) pilots, and digital approaches based on pilot subcarriers or blind estimation methods. The former ones insert a RF pilot tone into the OFDM spectrum and this pilot carrier is extracted at the receiver for carrier recovery [3, 4]. They require frequency guard bands and power overheads, thus reduce the spectral efficiency. The digital approaches include non-blind pilot aided (PA) methods [5] and blind methods [6]. PA methods are the most widely considered CPE compensation methods, due to their inherent advantages in both simplicity and accuracy. Nevertheless, they occupy a number of subcarriers, which reduce the spectral efficiency, especially in the cases of higher-order modulation formats. Blind methods do not need additional overheads but usually suffer from the cycle slip problem, and thus degrade the tolerance against the laser phase noise [5].

For an OFDM symbol, all the quadrature amplitude multiplexing (QAM) points contained in the constellation diagram can be treated as a planar graph over an I-Q plane. This provides a possibility that image processing methods may be feasible and effective to process the digital signal. In the presence of CPE, the constellation diagram of an OFDM symbol may be skewed. In our recent work [7], we reported our first proposal of adopting an image processing technique, named as minimum bounding box (MBB) method, so as to search for an axis-aligned bounding box with the minimum box area, which encloses all the QAM points on the I-Q plane in one OFDM symbol. With blind phase searching, the retrieved orientation of the minimum bounding box accurately implies the skew of the constellation diagram, induced by CPE. Hence, the CPE can be accurately estimated and compensated. Verified by numerical simulations and experiments, it has been shown that the MBB method has achieved comparable performance as the commonly used PA methods, with a drastically reduced overhead in the spectrum. However, the MBB based method requires phase searching, which involves extensive complex multiplications in the rotation procedure. Moreover, better accuracy of the phase estimation requires more test phases, but increasing the number of test phases requires more computation resources. In [8], we have further proposed a new geometric method to calculate the common phase error, which is named as best-fit bounding box (BBB) algorithm. The best-fit bounding box is defined as the minimum rectangle covering all the constellation points, which is not necessarily aligned to either vertical or horizontal axes. Based on the convex hull of the constellation points, the optimum best-fit bounding box can be found through the rotating calipers algorithm. Compared with the MBB method, there is no need to have blind phase searching in which all the constellation points are involved. Therefore, the computation complexity is further reduced. A preliminary proof-of-concept optical back-to-back experiment has been conducted in [8].

In this paper, we perform extensive characterization and comparison including a detailed theoretical analysis for the BBB method we proposed in [8]. The root mean square error (RMSE) is analyzed through numerical simulations to investigate its tolerances to both

Optics EXPRESS

channel noise and laser phase noise. Moreover, a modified BBB (mBBB) method is proposed to increase the tolerance against both the linear and nonlinear noises. Besides, a detailed complexity analysis is made among these CPE algorithms. Finally, an 840-km fiber transmission has been conducted to show the feasibility of the proposed BBB method as well as the mBBB method. The bit error ratio (BER) performance of the PA, MBB, BBB, and mBBB methods are compared through experiments.

The paper is organized as follows. Section 2 illustrates the principles of the proposed BBB algorithm and the modified BBB method. Detailed performance analysis is conducted in Section 3. Section 4 depicts the setup of the validation experiment, in details. In Section 5, the BER performance comparison between the PA method, the MBB method and the BBB method is discussed. Their noise tolerances against both linear and nonlinear noise are also addressed. Finally, Section 6 summarizes the paper.

2. Best-fit bounding box algorithm

At the receiver of a CO-OFDM system, after the coherent detection and conventional demodulation procedures, the k-th subcarrier in the i-th received OFDM symbols in time domain can be expressed as [5],

$$y_{ik} = x_{ik} \cdot h_k \cdot \exp(j\varphi_i) + n_{ik} \tag{1}$$

under the assumption that both frequency and timing are perfectly synchronized. In Eq. (1), the common phase error φ_i is independent of the subcarrier indices and remains constant in the duration of one OFDM symbol. h_k is the channel impulse response and n_k is the additive Gaussian white noise in the channel. The constellation diagram in Fig. 1(a) illustrates the noise effect on the received samples after the compensation of the channel response h_k. The common phase error φ_i induces common rotation to all the subcarriers in the OFDM symbol and thus the constellation diagram is skewed if we treat it as an image.

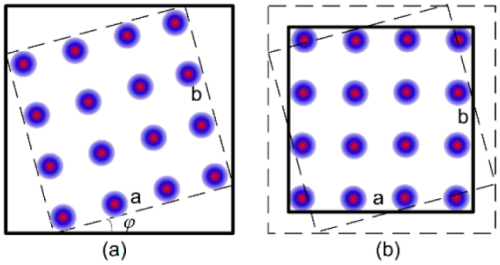

Fig. 1. Bounding box (solid line) of (a) a skewed rectangle and (b) a skew corrected rectangle.

To use image processing techniques to estimate the common phase error φ_i, we first construct the 2-D points set X_i, using the real part and the imaginary part of the samples y_{ik} in the i-th OFDM symbol.

$$\left(\Re\{y_{ik}\}, \Im\{y_{ik}\}\right) \in X_i, \tag{2}$$

where $\Re\{.\}$ and $\Im\{.\}$ denote the real and the imaginary part, respectively. The axis-aligned bounding box of a two-dimensional (2-D) graph is defined as the minimum rectangle in the horizontal and vertical direction (or axis-aligned) that covers all the pixels of the graph [9]. Figure 1(a) shows the axis-aligned bounding box (solid line) of a skewed rectangle with a rotated angle of φ, while the solid line in Fig. 1(b) shows the axis-aligned bounding box after the skew is corrected. It is intuitive that the area of the bounding box is a function of the rotated angle φ,

Optics EXPRESS

$$s = ab + \frac{a^2 + b^2}{2}\left|\sin\left(2\varphi\right)\right| \tag{3}$$

where a and b are the respective length and width of the original rectangle without skew. Figure 2 plots the normalized areas of the bounding boxes of different QAM orders with squared constellations, including 4-QAM (QPSK), 16-QAM, and 64-QAM, oriented at different rotated angles. All of them exhibit the same periodic curve with a period of π/2, and reach their minimum areas when the rotated angle equals $n \cdot \pi/2$, where n is an integer including 0, as shown in the dashed dot line in Fig. 2. Figure 2 also shows the cases for non-perfect rectangular constellation shape, say 32-QAM (in blue dashed line) and 128-QAM (in red solid line), and it is noticed that their minimum areas occur when the respective rotated angles are integer multiples of π/2, as well. The only difference is that their maximum areas do not occur at $\varphi = \pi/4$.

Now the estimation of CPE is formulated as finding the angle that minimizes the area of the axis-aligned bounding box of the constellation diagram. MBB method proposed in [7] is using the phase searching to approach the accurate estimation.

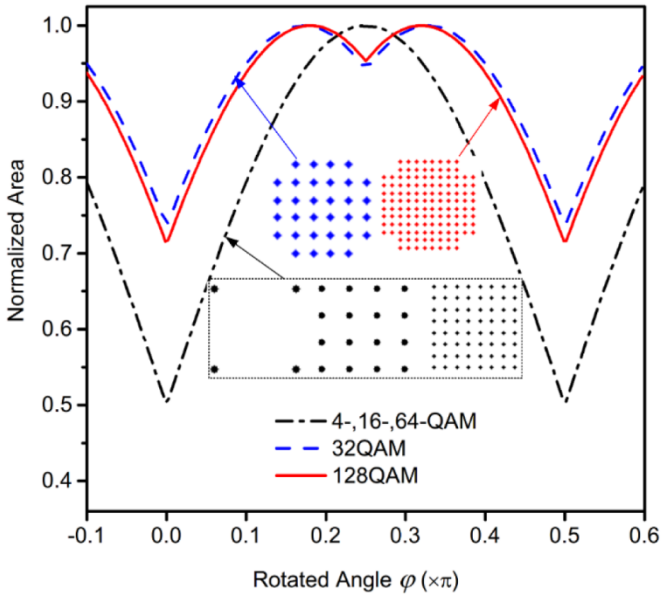

Fig. 2. Normalized area of bounding box w.r.t. the rotated angle in the constellation diagram of 4-, 16-, 32-, 64- and 128-QAM.

2.1 Principle of best-fit bounding box (BBB) method

Unlike the conventional definition of bounding box proposed in [7] which is limited to the upright direction, the best-fit bounding box is defined as the minimum rectangle that covers all the pixels in the graph in any possible direction. The rectangle in Fig. 3(a) depicts the best-fit bounding box of a points set in the plane. It can be obtained through the convex hull of these points. In computational geometry, the 2-D convex hull of a finite point set X_i is the smallest 2-D convex polygon that contains X_i. For instance, the points connected by the red solid line in Fig. 3(b) are the corresponding convex hull of these points. It has been theoretically proven that the smallest enclosing rectangle of a polygon has a side collinear with one of the edges of its convex hull [10].

The rotating calipers algorithm [11] is used to find the best-fit bounding box dependent on the convex hull. Each edge of the convex hull is rotated and aligned along a major axis, say x-axis. Next, the axis-aligned bounding box of the rotated convex hull is obtained, as illustrated

Optics EXPRESS

in Fig. 3(c), and its area is calculated. After applying the same procedures to all edges of the convex hull, the case with the minimum area is selected and the respective rotated angle from the initial state is the estimated CPE angle, as depicted in Fig. 3(d), for example.

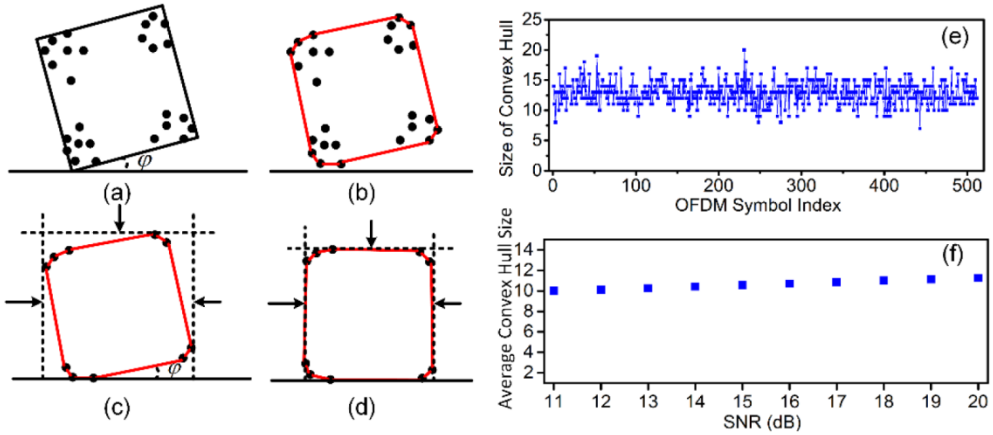

Fig. 3. Principles of using best-fit bounding box to estimate the common phase error. (a) Constellation diagram of the received block and its best-fit bounding box; (b) the convex hull of the constellation points (connected through red solid line); (c) rotate the convex hull by each slope angle and use caliper to calculate area for one certain slope angle; (d) the case when the minimum axis-aligned bounding box area is found; (e) the sizes of convex hull in each OFDM symbol with 128 data subcarriers; (f) the average sizes of the convex hulls of 50000 OFDM symbols with different SNR.

Compared with the previously proposed MBB method, the proposed BBB method has achieved reduced computation complexity and improved accuracy. In the MBB method, all the constellation points were rotated under each test phase and the respective bounding box's area was calculated. The required hardware resources increased linearly with the number of test phases, especially when higher order QAM signals were considered. However, in the proposed BBB method, only the points on the convex hull are involved in the rotation, thus the requirements for the real adders and multiplexers can be largely reduced. In this case, the total number of rotations is determined by the size of the convex hull, which refers to the number of edges that the convex hull contains, and is usually a small number, due to the limited total number of points on the convex hull.

Figure 3(e) plots the sizes of the convex hulls of 512 OFDM symbols, and each symbol has 128 data subcarriers loaded with 16-QAM symbols. The convex hull size ranges from 7 to 20, and has a mean value of 12.87 with a standard deviation of 1.90. Meanwhile, Fig. 3(f) shows the average sizes of the convex hulls of 50000 OFDM symbols under different signal-to-noise ratio (SNR) value. It shows that the size of convex hull is not sensitive to the noise level. Therefore, the adders and multipliers used in the rotation in the BBB method is much reduced compared with those in the MBB method. The most computation-intensive process of the BBB algorithm is the calculation of convex hull, which will be discussed in detail later in Section 3.2.

In general, the proposed BBB method offers a much improved option for CPE estimation and compensation in optical OFDM systems. Its operation principle is quite different from that of the previous MBB method [7]. In particular, it does not involve blind phase search and only a limited number of points on the convex hull of the data samples are involved in the computation. As the expected size of the convex hull of a square constellation is only $\log_2(N)$ [12], where N is the number of data samples, it requires much reduced computation complexity than the previous MBB method.

Optics EXPRESS

2.2 Modified BBB (mBBB) method

When using the bounding box based methods to correct the skew angle, one challenging factor that may influences the accuracy is the possible presence of outliers, which are defined as the sampled points that lie distant from the outermost constellation symbols. It may be attributed to the random properties of the amplified spontaneous emission (ASE) noise or the phase noise induced high-order effect, i.e., inter-channel interference, in optical transmission systems. For instance, Fig. 4(a) shows a few outliers (marked inside red circles) on the 16-QAM constellation diagram and they will be involved in the generation of the convex hull. After applying the BBB method, the constellation diagram can still be de-skewed, as shown in Fig. 4(b), thus the effects of these outliers are insignificant. However, for the case depicted in Fig. 4(d), the presence of the outliers (marked inside red triangles) severely affects the CPE estimation using the BBB method and large estimation error is observed, as shown in Fig. 4(e). Therefore, the outliers have to be removed to increase the estimation accuracy.

In [13], Rossen et al. discussed several algorithms for the optimal outlier removal based on different criteria, including minimizing diameter, enclosing rectangle, and enclosing convex hull. However, the complexities of these algorithms are relative high for our application thus not suitable for real-time implementation. Here, we propose a simplified method similar to the minimizing enclosing rectangle approach in [13], named as modified BBB (mBBB) method.

After applying the BBB method on the input constellation diagram, the points located in the four regions defined by

$$\begin{aligned}&\{P_1(x,y)\,|\,\alpha x_{\max} \le x \le x_{\max}\}, \{P_2(x,y)\,|\,x_{\min} \le x \le \alpha x_{\min}\},\\ &\{P_3(x,y)\,|\,\alpha y_{\max} \le y \le y_{\max}\}, \{P_4(x,y)\,|\,y_{\min} \le y \le \alpha y_{\min}\}\end{aligned} \tag{4}$$

will be checked, where x and y are the real and imagine part of the constellation points respectively, α is a coefficient which is optimized as 0.98 in our simulation. The numbers of points in these four regions could be used as an estimation of the density. If the points in any region are less than a threshold number (2 was used in our work), this region is judged as containing outliers and all the points in this region are removed then another BBB procedure is performed. Otherwise, there are no outliers thus there is no need to perform additional BBB process. Figures 4(b) & 4 (e) illustrate the denoising process of the mBBB method.

Meanwhile, the ASE and inter-channel interference both have a Gaussian distribution of constellation points. As long as 1-α is not too big, this process is reliable to improve the performance. Figures 4(c) and (f) show the constellation diagrams after applying the edge de-noising algorithm. The outliers are successfully removed and the CPE in both cases are compensated perfectly. One step of the edge denoising procedure in mBBB is enough due to the relatively large noise tolerance of the BBB algorithm.

It is worth noting that the ambiguity problem in [7] is also a critical issue in the BBB algorithm. Therefore, a two-bit quasi-pilot is still necessary here. The quasi-pilot design is the same as in [7].

Optics EXPRESS

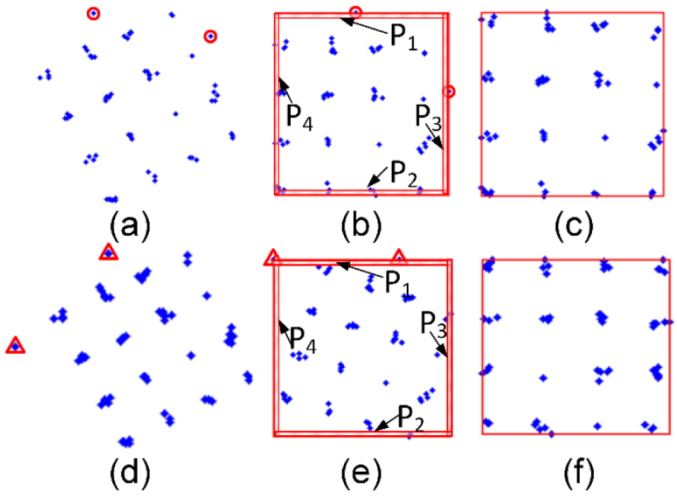

Fig. 4. Illustration of outliers in the constellation diagram. (a) & (d) outliers in a 16-QAM constellations (circle and triangle); (b) & (e) the de-skewed constellation diagrams and their bounding boxes via BBB method; (c) & (f) the constellation diagrams after applying edge de-noising algorithm.

3. Performance analysis

In this part, we investigate the performance of the proposed best-fit bounding box method. The noise tolerance, including the robustness to ASE noise and the variance of laser phase noise, which is characterized by laser linewidth, is investigated in detail. Moreover, a comprehensive analysis of the computation complexity has been made to take the practical implementation into consideration.

3.1 Noise tolerance

To have an accurate CPE estimation using image processing technique, sufficient samples are required to obtain a reliable bounding box. Similar to the PA method, the number of data samples in one OFDM symbol contributes to the estimation accuracy and the noise tolerance. Here, we performed numerical simulations to investigate the noise tolerance with the different numbers of samples used in the CPE estimation. One million OFDM symbols with an fast Fourier transform (FFT) size of 256 was generated. 120 of the subcarriers were modulated with 16-QAM data. The phase noise was added by multiplying the time-domain symbols with the phase noises which have a random distribution under Wiener-Levy process [2]. At the receiver, N samples with equal spacing were used to form the 2-D constellation graph and estimate the CPE.

Figure 5(a) shows the simulation results of the root mean square error (RMSE) of CPE estimation for 16QAM-OFDM signal using the MBB and the BBB methods under the same SNR range, respectively. The mean value of the phase noise in one OFDM symbol duration was used as the CPE reference. The value of N was changed from 20 to 120 in both cases. It showed that if more samples in the OFDM symbol were used to estimate the CPE, the RMSE could be reduced in both MBB method and the BBB method, and the noise tolerance was increased as well. In most cases, less than 0.1 rad of RMSE could be achieved when the SNR was higher than 10 dB. It was also shown that the BBB method achieved a lower average RMSE than the MBB method, indicating the increased accuracy. Figure 5(b) shows that the mBBB method could further reduce the RMSE of CPE estimation significantly, especially when more data samples were used.

Optics EXPRESS

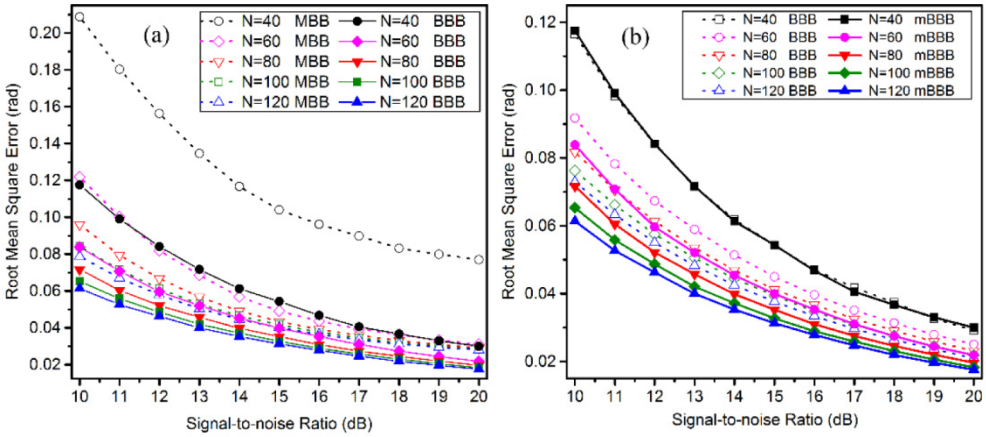

Fig. 5. (a) Root mean square error of CPE estimation under different signal-to-noise ratio. N is the number of samples involved in the calculation of CPE using MBB method. The number of test phases used in MBB method is 20. (b) Root mean square error of CPE estimation under different signal-to-noise ratio. *N* is the number of samples involved in the calculation of CPE using BBB method.

Another noise effect that may limit the performance of the proposed CPE estimation methods is the variance of laser phase noise, characterized by the laser linewidth. We have compared the tolerance against the laser phase noise for both QPSK-OFDM and 16QAM-OFDM signals, via simulations. The results, as depicted in Fig. 6, showed very similar laser linewidth tolerance among the cases of PA method, MBB method, and BBB method with or without edge de-noising.

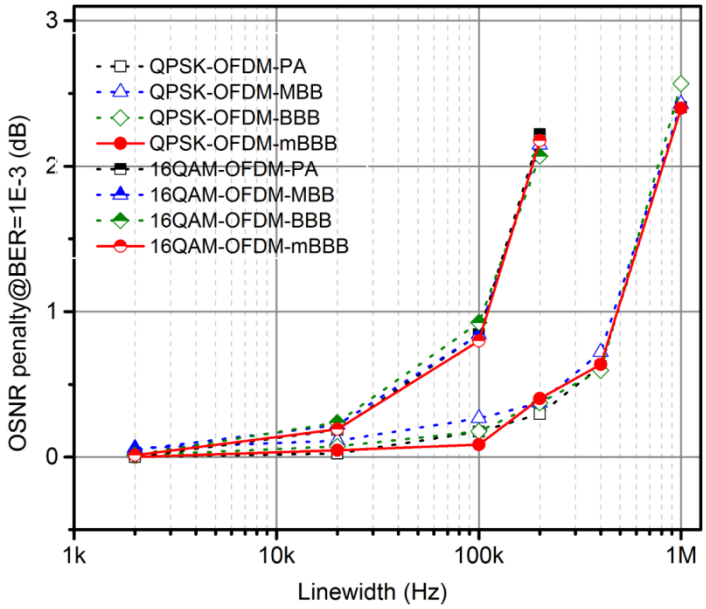

Fig. 6. OSNR penalty at BER = 10^{-3} for PA, MBB, BBB and mBBB algorithms, under different laser linewidths.

3.2 Computation complexity

With the help of pilot subcarriers, the pilot-aided method does not require much computation. At the receiver, the phases of the pilot subcarriers are averaged as the estimation of common

Optics EXPRESS

phase error. On the other hand, the minimum bounding box (MBB) method in [7] can be regarded as a modified blind phase searching (BPS) method [14], which is a commonly used carrier phase recovery algorithm in the single-carrier system.

In the proposed BBB methods, after the convex hull is obtained, the rotating calipers technique has a similar complexity behavior as in the previously reported MBB method, but with much reduced (up to ~10 times) required number of data samples, as discussed in Section II. However, the major complexity lies in the calculation of convex hull. Fortunately, as a key enabling algorithm in most image processing techniques, the calculation of convex hull has been well investigated and the complexity has been reduced to O(N*log(N)) via Graham Scan Algorithm [15] or even O(N*log(H)), via Chan's algorithm [16] if the expected number of points in the convex hull H is preset. For a typical square constellation diagram, the expected H could be approximated as $\log_2(N)$ [12]. In the Graham Scan Algorithm, there is an initial radial sorting process which needs a so-called "is-left" decision to decide whether one point is in the counter-clock or clock-wise direction of the line determined by the origin and the previous point [15]. Equation (5) gives the implementation of the "is-left", showing how to determine the position of P_2 and P_0P_1, where (x_i, y_i) is the coordinates of the point of P_i. If the determinant Δ is positive, it means P_2 is on the left of the line of P_0P_1, while a negative Δ shows that P_2 is on the right of the line of P_0P_1,.

$$\Delta = (x_1 - x_0)(y_2 - y_0) - (y_1 - y_0)(x_2 - x_0) \tag{5}$$

As seen in Eq. (5), this "is-left" process consists of 5 real additions and 2 real multiplications. The initial sorting can be finished with at most $N \times \log(H)$ steps, after which each point is checked to determine whether it is in the convex hull by the same "is-left" calculation. In this step, each point is processed twice at most. Hence, $N \times \log(N) + 2N$ "is-left" operations are required in total in the worst case. Chan's algorithm can speed up this process to be $N \times \log(H) + 2N$, in which the preliminary process is also the same "is-left" operation. The mBBB algorithm needs more comparators and one more BBB procedure if the outliers are found in the current convex hull. Table 1 shows the comparison of the hardware computation complexities among the proposed BBB algorithms, PA, MBB and blind phase searching (BPS) methods. The hardware requirement in the worst case of the aforementioned CPE algorithms is also listed in Table 1, where K is the number of pilot subcarriers; M is the number of samples in one OFDM symbol; B is the number of test phases in BPS and MBB; and H is the expected size of convex hull.

Table 1. Hardware Complexity Comparison

Methods	Multiplexer	Adder	Comparator	Decision
PA	*2*	*2K*	*0*	*0*
BPS	*6M·B + 4M*	*6M·B-B + 2M + 2*	*M·B*	*M·B + M*
MBB	*4M·B + 4M + B*	*2M·B + 2B + 2M*	*4M·B + B*	*0*
BBB	*5M(log(H) + 2) + 4H·H + H + 4M*	*2M(log(H) + 2) + 3H·H + H + 2M*	*3M + 3H·H*	*0*
mBBB	*2BBB_multi*	*2BBB_adders*	*2BBB_camp + 8M*	*0*

To be more specific, in our simulations and experiments, $M = 128$, $B = 16$, $H = 16$. Then the number of real multiplexers used in BPS, MBB, BBB and mBBB methods are 12800, 8720, 5392, and 9880, respectively. Meanwhile, the number of real adders used in BPS, MBB, BBB and mBBB are 12530, 4384, 2576 and 4472, respectively. It is clearly seen that the newly proposed BBB methods have 38.17% and 41.24% reduction in the requirement of real multiplexers and adders compared with the previous MBB method. Due to the additional BBB process, mBBB requires a little more hardware resource than the MBB method in the worst case, but still much less than that requires in the BPS method. It is worth noting that if the number of points in one OFDM symbol is large enough, an order of magnitude reduction in the convex hull computation time can be achieved [9]. Moreover, a simple pre-processing heuristic is often used to further largely reduce the data calculations involved in the convex

Optics EXPRESS

hull calculation [17]. Hence, an expectation of linear processing time has been achieved in [18].

4. Experiments

Figure 7 shows the experimental setup to verify the proposed CPE estimation schemes. The size of inverse fast Fourier transform (IFFT) was 256. Pseudo random binary sequence was mapped to 16-QAM symbols and loaded into 128 subcarriers. 16 pilot subcarriers were equally inserted in the 128 data subcarriers. Another one quasi-pilot subcarrier using the aforementioned mapping method was inserted in the front of the data subcarriers. The rest subcarriers were padded to be zero. The OFDM signal sequence was generated offline by a personal computer and loaded to an arbitrary waveform generator (Tektronix 7122C) to generate radio-frequency (RF) OFDM signal with a sampling rate of 12 GSample/s.

Two narrow-linewidth tunable lasers were used as the signal laser and the local oscillator, with the equal linewidth of ~100 kHz, resulting in an equivalent linewidth of ~200 kHz. The continuous wave from the signal laser was modulated with the RF OFDM signal, as described above, via an optical IQ modulator. The generated optical OFDM signal was first amplified by an Erbium doped fiber amplifier (EDFA), followed by a variable optical attenuator (VOA), so as to emulate different OSNR values. The optical signal was then fed into a recirculating loop, which comprised a segment of 70-km single mode fiber, followed by an EDFA to compensate the power loss in the loop. The received optical signal was detected by a conventional coherent optical receiver. The electrical signal was then sampled by a real-time oscilloscope (Tektronix 72004B) at a sampling rate of 50 GSample/s for offline digital signal processing. Conventional OFDM synchronization and frequency offset compensation method [19] were employed. The channel estimation was implemented through training sequences.

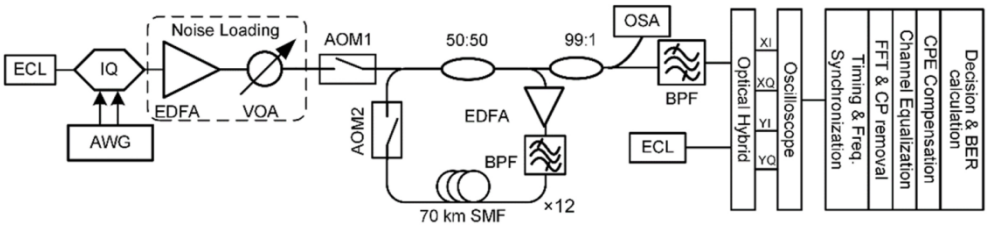

Fig. 7. Experimental setup. ECL: external cavity laser; AWG: arbitrary waveform generator; VOA: variable optical attenuator; AOM: acousto-optic modulator; OSA: optical spectrum analyzer; BPF: optical band-pass filter.

5. Results and discussion

First, we characterized the back-to-back (B2B) experiment. The bit error rate was calculated with different CPE methods at each optical-to-noise ratio (OSNR) value. The calculation of the convex hull of the data samples in OFDM symbol was implemented by the Chan's Algorithm [16] in the offline processing and the expected size of the convex hull was chosen to be 16. Figure 8(a) shows the BER versus OSNR using the common PA method with the number of pilot-aided subcarriers ranging from 2 to 16, as well as that employing BBB method to compensate CPE with and without modification. The result shows that the BBB method had a comparable performance as the PA method with 16 pilots. Using the same experiment data set, we applied the MBB method with the different number of test phases from 4 to 16 and the results were compared with that using the BBB method, as shown in Fig. 8(b). It could be clearly seen that the modified BBB method achieved the best performance. This could be attributed to that the BBB method does not have any limitation on the resolution, as discussed.

Optics EXPRESS

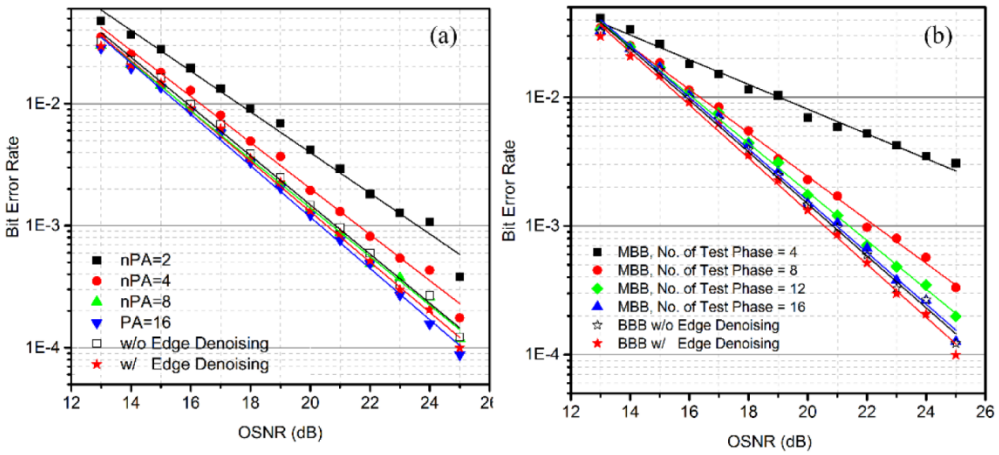

Fig. 8. (a) Bit error rate versus OSNR. PA and BBB methods are used. Numbers of pilot subcarriers (PS) used in PA method are 2, 4, 8, and 16 (b) Bit error rate versus OSNR. MBB and BBB methods are used. Numbers of test phase used in MBB method are 4, 8, 12, and 16.

To further investigate the tolerance of the proposed MBB and BBB methods against fiber nonlinearity, an 840-km transmission experiment was conducted. As seen in Fig. 9, the long-haul transmission was emulated, via a recirculation loop with 12 spans of 70-km single mode fiber. The input power into the recirculation loop was altered from −4 dBm to + 7 dBm, in a step of 3 dB. The Q-factors were calculated, using PA, MBB, and BBB methods, from 50000 OFDM symbols at each input power value. Figure 9 shows that the BBB method has a slight performance improvement in the linear regime while its nonlinear tolerance was slightly weak than the PA and MBB methods. However, when the modified BBB was applied, the Q-factor improvement was significant, which was about 0.08 dB better than that with BBB method. Compared with the PA method, the Q-factor improvement at −1 dBm input power was ~0.15 dB. The results showed that the proposed BBB method has a comparable performance as the common PA method.

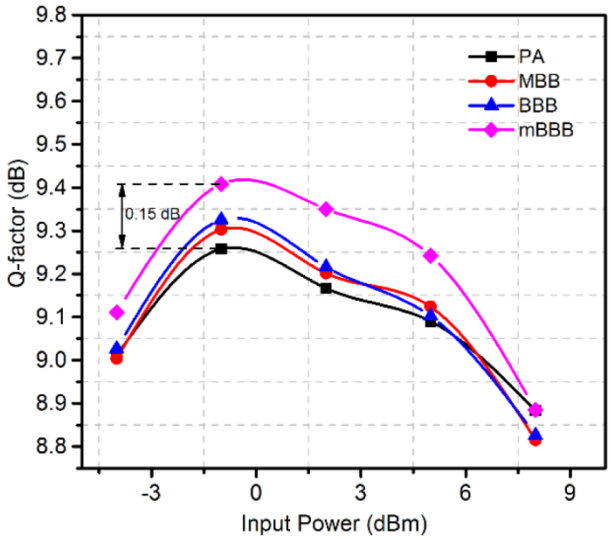

Fig. 9. Q-factor versus input power with PA method, MBB method, BBB method and mBBB method in 840-km single mode fiber transmission.

Optics EXPRESS

In general, conventional PA method has the least complexity, as it only calculates the phase average among all the pilot subcarriers. Nevertheless, our proposed BBB methods use a non-data-aided approach to achieve comparable performance and much increased spectral efficiency than the conventional PA method, but at an expense of increased computation complexity. The computations involved are the common process adopted in image processing and hardware implementation friendly.

6. Summary

We have characterized and evaluated the best-fit bounding box method for the common phase error estimation in coherent optical OFDM systems. A practical accuracy improvement method has been proposed and characterized, as well. Both numerical simulations and experiments have shown that the best-fit bounding box method can realize substantial improvement in the spectral efficiency and comparable performance, as compared with the common PA method.

Funding

Faculty of Engineering, The Chinese University of Hong Kong (Project ID: 3132822).